

Heat and Mass Transfer in the Nonisothermal Fixed Bed Adsorption Column

Chieko FUJINO

Abstract

The cell model approach for the analysis of nonisothermal fixed bed adsorption column has been presented under the assumption that adsorption is controlled by intraparticle diffusion and adsorption equilibrium is nonlinear. The numerical analysis has been carried out by the Runge-Kutta-Gill scheme. With the aid of a HITAC-8800 computer, the influences of controlling variables on the breakthrough curves and temperature curves have been made clear for such parameters as solid phase mass transfer coefficient, overall heat transfer coefficient at the column wall, length of bed and the equilibrium isotherms. The experimental results were compared with the computer prediction by this model and, after an adjustment of the values of mass transfer coefficient and overall heat transfer coefficient assumed, agreed well.

1. Introduction

Gas adsorption resembles the phenomenon of vapour condensation and usually generates the heat of adsorption which corresponds to that of condensation. Hence, bed temperature rises with the progress of adsorption. To predict the performance of a fixed bed adsorption column, one requires four basic differential equations on fluid phase mass balance, energy balance, appropriate mass transfer relation and equilibrium isotherms.^{1),2)} It is difficult, however, to obtain the solution of the foregoing simultaneous equations analytically. So the study has mostly been limited to the special cases of either isothermal operation^{3),4)} or adiabatic operation.^{5),6),7)} Currently, a large-diameter adsorption column is frequently utilized to treat of high concentration adsorbate. In this case, a large amount of heat of adsorption is generated and is not easily removed through the bed wall cooling. Also, industrial adsorption columns are generally operated with appreciable heat loss at the wall, so that conditions are neither truly isothermal nor adiabatic. So the performance of a nonisothermal fixed bed adsorption column is necessary but is hard to solve analytically. From that it follows, a mathematical treatment which is based on the cell model is presented to obtain theoretical breakthrough curve and temperature curve numerically for the nonisothermal fixed bed adsorption column. And theoretical solutions were compared with the experimental results of M.S.5A-CO₂ system to estimate overall heat transfer coefficient and mass transfer coefficient.

2. Theory

A fixed bed is regarded as a number of perfectly mixed cells in series^{8),9),10)} as shown in **Fig. 1**. Each cell has the constant cross sectional area S and the constant height L_0

Received September 27, 1978

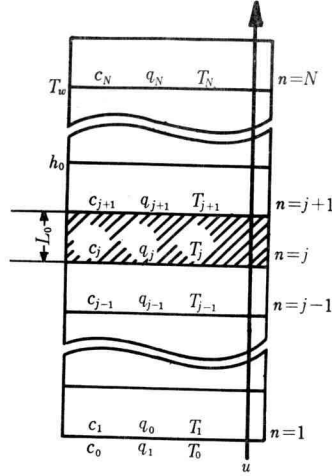


Fig. 1 Schematic diagram of Cell Model

which equals to the average length of one adsorbent particle. The concentration, temperature and adsorbate loading in each cell are uniform. The following assumptions are used to formulate the simplified model.

1. There are no temperature or concentration gradients along the bed radius.
2. Pressure loss is negligible in the bed, and superficial velocity is assumed constant.
3. C_{pg} , C_{ps} , ρ_g , ΔH , $k_s a_p \gamma$ and h_0 are constant throughout the operation and independent of temperature.
4. The wall temperature equals the external temperature and is constant throughout the operation.
5. Adsorbent particles are thermally in equilibrium with the fluid.
6. Local overall mass transfer between particles and fluid is governed by intraparticle diffusion.

With these assumptions, the relevant ordinary differential equations are as follows.

Mass balance:

$$\frac{u\epsilon(c_j - c_{j-1})}{L_0} + \epsilon \frac{dc_j}{dt} + \gamma \frac{dq_j}{dt} = 0 \quad (1)$$

Energy balance:

$$\begin{aligned} \frac{u\epsilon \rho_g C_{pg} (T_j - T_{j-1})}{L_0} + (\epsilon \rho_g C_{pg} + \gamma C_{ps}) \frac{dT_j}{dt} \\ + \gamma \Delta H \frac{dq_j}{dt} + \frac{4}{D} h_0 (T_j - T_w) = 0 \end{aligned} \quad (2)$$

Rate equation:

$$\frac{dq_j}{dt} = k_s a_p \gamma (q_j^* - q_j) \quad (3)$$

The equilibrium isotherm is generally given as a function of temperature and adsorbate concentration.

$$q_j^* = q^*(c_j, T_j) \quad (4)$$

For calculation, however, it is necessary to formulate an isotherm more definitely. So, being the isotherm of M.S. 5A-CO₂ system approximated by Langmuir equation, one assumes that equilibrium is governed by a Langmuir isotherm to compare the experimental results with the computer results. Then Eq. (4) becomes Eq. (5).

Equilibrium isotherm:

$$q_j^* = \frac{a_j b_j c_j}{1 + a_j c_j} \quad (5)$$

$$\text{where } a_j = a_0 \exp\left(-\frac{\Delta H}{RT_j}\right)$$

$$b_j = b_1 - b_2 T_j$$

Another isotherms such as Dubinin-Astakov's type¹¹⁾ or linear type have been used and solutions have been obtained¹²⁾, but one doesn't touch up them in this paper.

Eqs. (1)–(3) and (5) are the fundamental equations for analyzing the nonisothermal fixed bed adsorption columns which subjects to the initial and boundary conditions as follows.

Initial conditions:

$$c_j = q_j = 0 \quad \text{and} \quad T_j = T_0 = T_w \quad \text{at } t = 0 \quad (6)$$

Boundary conditions:

$$c_j = c_0, \quad q_j = 0 \quad \text{and} \quad T_j = T_w \quad \text{at } j = 0 \quad (7)$$

To obtain the solution of these simultaneous equations, let us transform Eqs. (1)–(3) and (5)–(7) into Eqs. (8)–(13) in dimensionless forms.

Dimensionless mass balance:

$$\frac{x_j - x_{j-1}}{h} + \frac{dx_j}{d\tau} + \delta \frac{dy_j}{d\tau} = 0 \quad (8)$$

Dimensionless energy balance:

$$\frac{\theta_j - \theta_{j-1}}{h} + \nu \frac{d\theta_j}{d\tau} + \mu \frac{dy_j}{d\tau} + \omega \theta_j = 0 \quad (9)$$

Dimensionless rate equation:

$$\frac{dy_j}{d\tau} = \kappa (\eta_j - y_j) \quad (10)$$

Dimensionless equilibrium isotherm:

$$\eta_j = \frac{(1 - \beta \theta_j) x_j \exp\left(\frac{\lambda \theta_j}{1 + \theta_j}\right)}{r + (1 - r) x_j \exp\left(\frac{\lambda \theta_j}{1 + \theta_j}\right)} \quad (11)$$

Dimensionless initial conditions:

$$x_j = y_j = \theta_j = 0 \quad \text{at } \tau = 0 \quad (12)$$

Dimensionless boundary conditions:

$$x_j = 1.0 \quad y_j = \theta_j = 0 \quad \text{at } j = 0 \quad (13)$$

Dimensionless terms and coefficients which are used for the above mentioned transformation are defined as follows:

$$x = \frac{c}{c_0}, \quad y = \frac{q}{q_0^*}, \quad \eta = \frac{q^*}{q_0^*}, \quad (14)$$

$$\theta = \frac{T - T_w}{T_w}, \quad \tau = \frac{ut}{L}$$

and

$$h = \frac{L_0}{L}, \quad r = \frac{1}{1 + a_0 \exp\left(-\frac{\Delta H}{RT_0}\right) c_0}, \quad \beta = \frac{b_2 T_0}{b_1 - b_2 T_0}$$

$$\delta = \frac{\gamma q_0^*}{\varepsilon c_0}, \quad \kappa = \frac{k_s a_p \gamma L}{u}, \quad \lambda = \frac{\Delta H}{RT_0}, \quad (15)$$

$$\mu = \frac{\gamma \Delta H q_0^*}{\varepsilon \rho_g C_{pg} T_w}, \quad \nu = \frac{\varepsilon \rho_g C_{pg} + \gamma C_{ps}}{\varepsilon \rho_g C_{pg}}, \quad \omega = \frac{4 h_0 L}{Du \varepsilon \rho_g C_{pg}}$$

The breakthrough curve and the corresponding dimensionless temperature curve may be obtained, in terms of the parameters κ , ω , r and h by solving Eqs. (8)–(11) simultaneously with Eqs. (12) and (13). Solutions were obtained numerically for various values of the parameters, using a fourth order Runge-Kutta-Gill scheme. HITAC 8700–8800 at the computer center of the Univ. of Tokyo is used for these calculations.

3. Experimental Equipment and Procedure

The equipment is outlined in **Fig. 2**. N_2 was used as the carrier gas and CO_2 was used as the adsorbate. The packed bed consisted of copper column of 29.7 mm i.d. and 270 mm height. The column was enclosed in a circulating water thermostat which maintained the temperature of the column wall constant. Molecular sieve 5A pellets were packed to the column at the thickness about 20 mm. Operating temperature was at about 25°C, 40°C or 55°C. The conditions of the experimental runs are summarized more minutely in **Table 1**. Glass beads with the same diameter as that of the adsorbent were packed as the pre- and after-calming sections. Effluent gas concentration was detected by a thermal conductivity cell. The outlet temperature of the bed was the arithmetic mean of temperature readings of four chromel-alumel thermocouples placed radially at equal distance, where the first thermocouple was placed at the center and the fourth one was about 4 mm apart from the bed wall. Potentiometric recorder was incorporated to monitor continuously the thermocouple outputs.

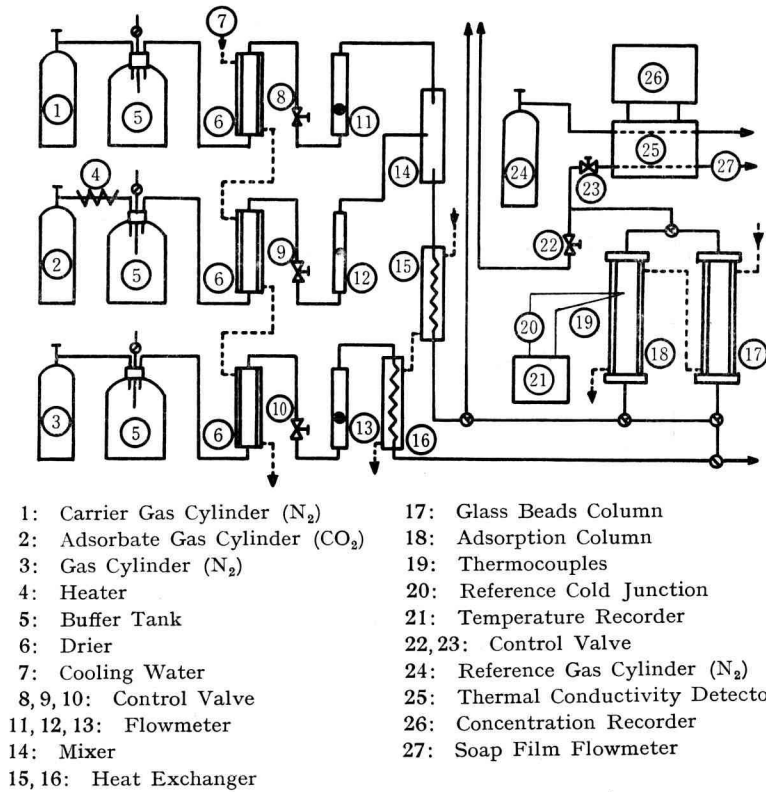


Fig. 2 Schematic diagram of experimental equipment

Table 1 Experimental Conditions

Run	d_p [cm]	L [cm]	γ [g/cm ³]	ε [—]	f_0 [—]	$c_0 \times 10^4$ [g/cm ³]	T_w [°C]	u [cm/sec]	Re_p [—]	q_0^* [g/g _{ad}]
1	0.200 (1/16")	1.88	0.681	0.375	0.2	3.60	25.0	9.62	16.8	0.131
2		2.12	0.672	0.384		3.61	24.1	10.0	14.9	0.132
3		2.18	0.635	0.417		3.61	23.8	10.4	15.5	0.132
4		2.18	0.679	0.377		3.62	23.7	12.1	18.1	0.133
5		2.40	0.686	0.371		3.60	25.0	13.0	22.7	0.131
6		2.09	0.710	0.349		3.44	38.5	11.0	15.2	0.116
7		2.05	0.710	0.349		3.44	38.6	12.4	17.1	0.116
8		2.09	0.709	0.350		3.27	55.2	11.0	14.0	0.0955
9		2.05	0.734	0.327		3.27	55.0	13.2	16.9	0.0958
10	0.423 (1/8")	4.44	0.663	0.392	0.1	3.61	24.2	9.21	29.0	0.132
11		4.36	0.668	0.387		3.60	24.6	9.95	31.3	0.132
12		4.28	0.645	0.408		3.61	24.0	11.8	37.2	0.132
13		2.28	0.670	0.385		3.61	24.2	10.0	31.5	0.132
14		2.26	0.672	0.383		3.61	24.0	12.6	39.6	0.132
15		4.37	0.670	0.386		1.81	24.0	9.99	29.2	0.123
16		4.12	0.677	0.379		1.80	24.3	11.4	33.4	0.122

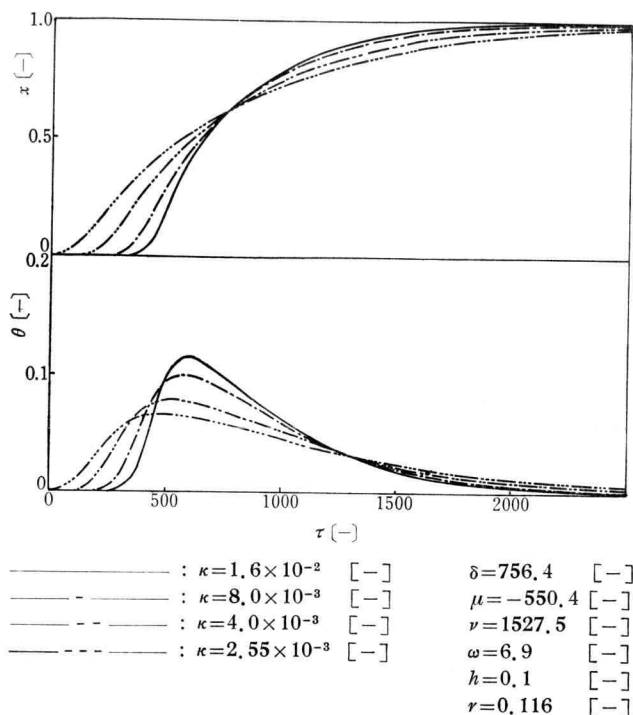


Fig. 3 Theoretical breakthrough curves and temperature curves showing the effects of κ

4. Results and Discussion

4-1. The effects of κ on the numerical solutions

Fig. 3 shows the effects of κ , dimensionless mass transfer coefficient, upon the theoretical breakthrough curves and temperature curves. As κ increases, intraparticle residence decreases and mass transfer takes place easily. So the spread of breakthrough curve decreases with longer lag time. As a result, the appearance of temperature rising point is delayed. Moreover, as κ increases, a large amount of heat of adsorption is generated for a short time because of the large efficiency of adsorption. Thus, temperature curve becomes steeper at the transition region and maximum temperature becomes higher.

4-2. The effects of ω on the numerical solutions

Fig. 4 shows how dimensionless heat transfer coefficient ω influences the bed performance, where $\omega=0$ and $\omega=\infty$ correspond to adiabatic case and isothermal case, respectively. The heat loss through the bed wall decreases, as ω decreases. Also the outlet temperature rises rapidly, reaching the maximum and decreasing slowly thereafter. As a result, the bed starts to breakthrough earlier, the slope of the breakthrough curve becomes steeper at the transition region and the increase of slope becomes smaller after reaching the maximum temperature. In the case of small value of κ , this tendencies aren't recognized clearly. But

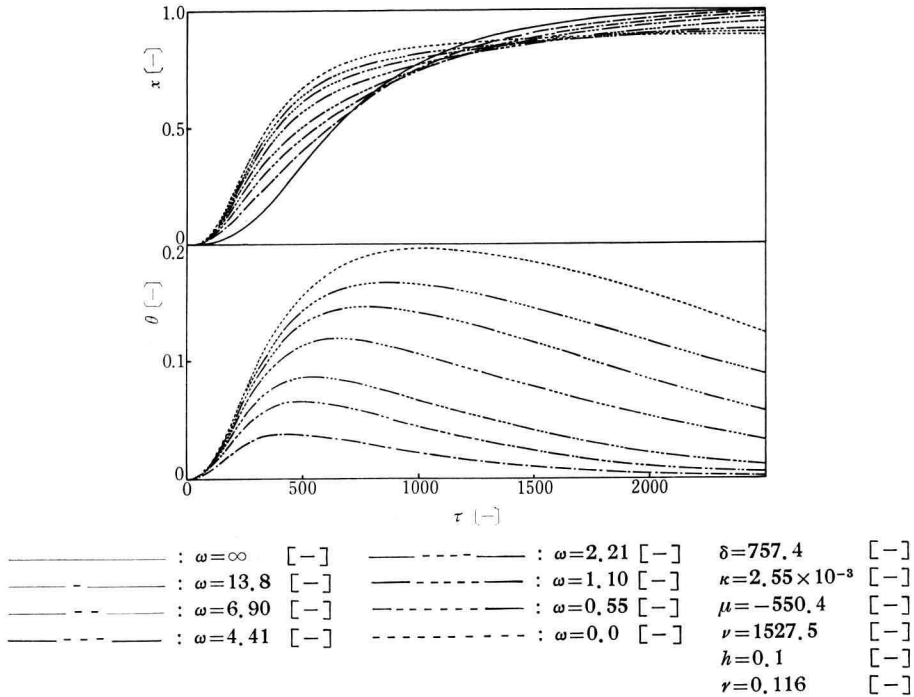


Fig. 4 Theoretical breakthrough curves and temperature curves showing the effects of ω

Fig. 5, with large value of κ , shows distinctly that as κ decreases, lag time becomes shorter and the spread of breakthrough curve decreases. Thus, a column with smaller ω shows the delay of breakthrough, especially in the case with large value of κ , when the column is designed under the assumption of isothermal operation.

4-3. The effects of r on the numerical solutions

The effects of r -equilibrium parameter – is illustrated in **Fig. 6**. As r decreases, the lag time becomes longer and the spread of temperature curve decreases with higher maximum temperature. But the spread of breakthrough curve increases. This is different from the isothermal case. As r approaches zero, nonlinearity of the isotherm increases and the system approaches irreversible isotherm. So transfer zone becomes shorter and adsorption can be carried out more effectively. Thus in the isothermal case which has no effect of accumulated heat, as r decreases, the lag time becomes longer and the spread of breakthrough curve decreases. But when it is impossible to neglect the effect of generated heat, that is in the nonisothermal case, as r decreases, the generated heat increases owing to the increase of the facility of adsorption. Thus the spread of breakthrough curve increases at the latter stage of adsorption, after reaching the maximum temperature, where a large amount of heat is accumulated in the bed, as r decreases. It is found that the effects of accumulated heat become significant for the system with highly nonlinear isotherm.

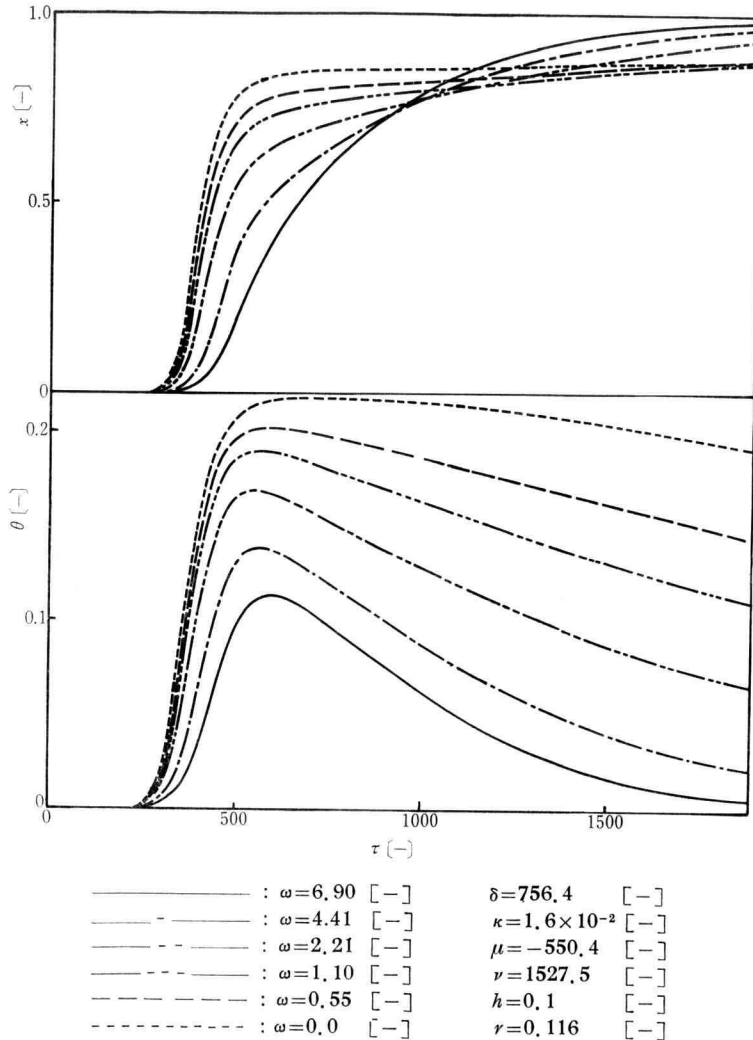


Fig. 5 Theoretical breakthrough curves and temperature curves showing the effects of ω

4-4. The effects of h on the numerical solutions

From **Fig. 7** it is seen that as h –dimensionless bed length– decreases, flow in the bed approaches piston flow and the spreads of both of the breakthrough curve and temperature curve decrease with longer lag time and higher maximum temperature. Moreover it is noticed that the theoretical curves are sensitive to the variation of parameter h while the value of h is from 1.0 to 0.05 (i.e. $n=1 \sim 20$), but when h is less than 0.05 (i.e. $n \geq 20$), theoretical curves are hardly influenced by the variation of h and approach an asymptotic curve.

When fixed bed is regarded as the perfectly mixed cells in series, it is necessary to use a

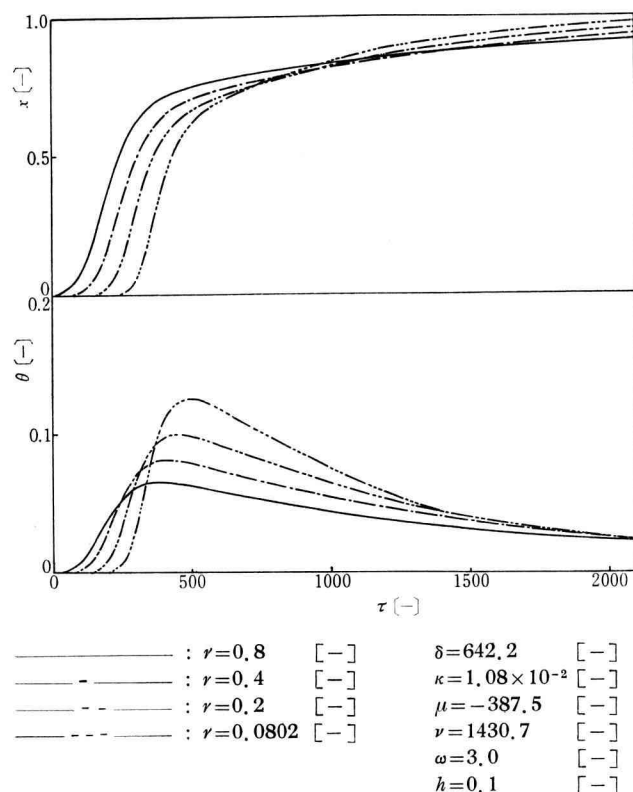


Fig. 6 Theoretical breakthrough curves and temperature curves showing the effects of r

particle diameter as a cell length. For analysis of a long adsorption column, therefore, a large number of cells is necessary and calculation time for simulation becomes much longer. This is a weak point of cell model. But, for a long column which have numerous cells—at least more than 20, that means h is less than 0.05—, it is possible to simulate by using a larger value of h than the one estimated by Eq. (15), because h has little effect on the theoretical curves in that case as stated above. This means that when one simulates a small size column, a particle diameter must be used as a cell length, but when a long column, one may use a larger length than particle diameter. As a result, great savings in time and money are achieved through the use of this length.

4-5. Comparison of the experimental results with the numerical solutions

Experiments using a shallow bed are carried out to shorten the calculation time. In order to compare the experimental data with the numerical results, one must determine the values of parameters represented by Eq. (15). The values of u , L , c_0 and T_0 are obtained by the experimental conditions. The values of ε and γ are estimated by the situation of filling in the bed. The values of ρ_g , C_{pg} and C_{ps} are obtained for certain values of c_0 and T_0 . Also

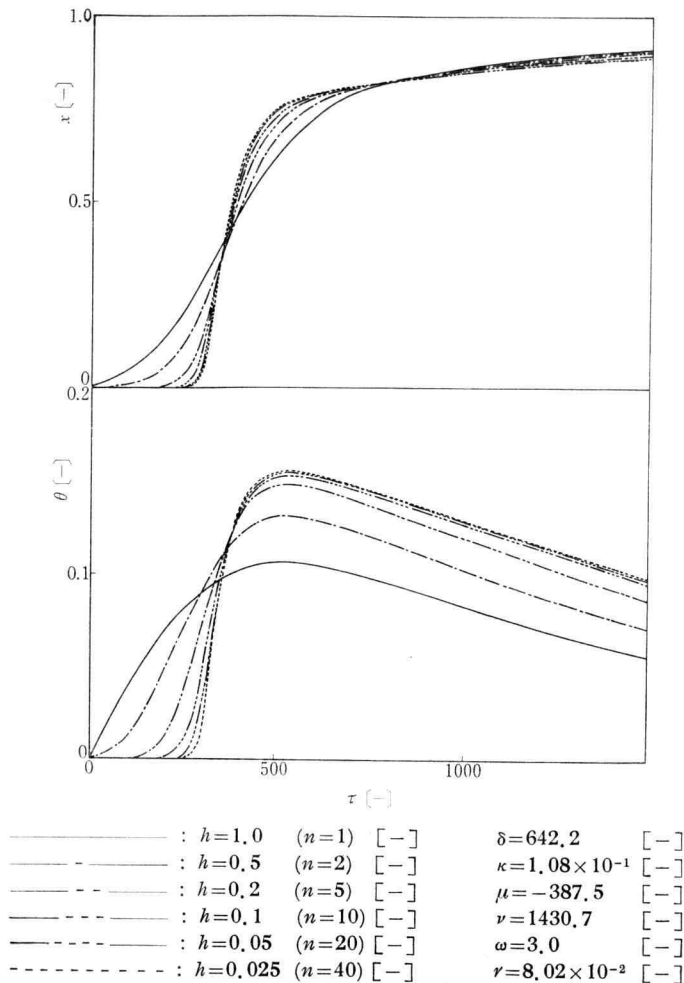


Fig. 7 Theoretical breakthrough curves and temperature curves showing the effects of h

q_0^* is determined. In this experiment the height of bed is so small that a particle diameter which is equivalent to sphere is used as a cell length. The values of ΔH , a_0 , b_1 and b_2 are found by fitting the isotherm to a Langmuir equation. R is the gas constant and known value. Then the values of parameter h , r , β , δ , ν , λ and μ are calculated. The values of κ and ω , however, which contain unknown values of k_s and h_0 respectively are difficult to estimate. A trial and error procedure is therefore employed to derive these parameters from the experimental breakthrough curve and temperature curve. The origin values of k_s and h_0 are estimated by the methods based on the theory of isothermal adsorption^{13),14)} and the theory of steady state heat transfer in the packed bed,^{15),16),17)} respectively. Fig. 8 is an example of the comparison of numerical solution with the experimental results. The values of k_s and h_0 are estimated from κ and ω which give the best agreement with the

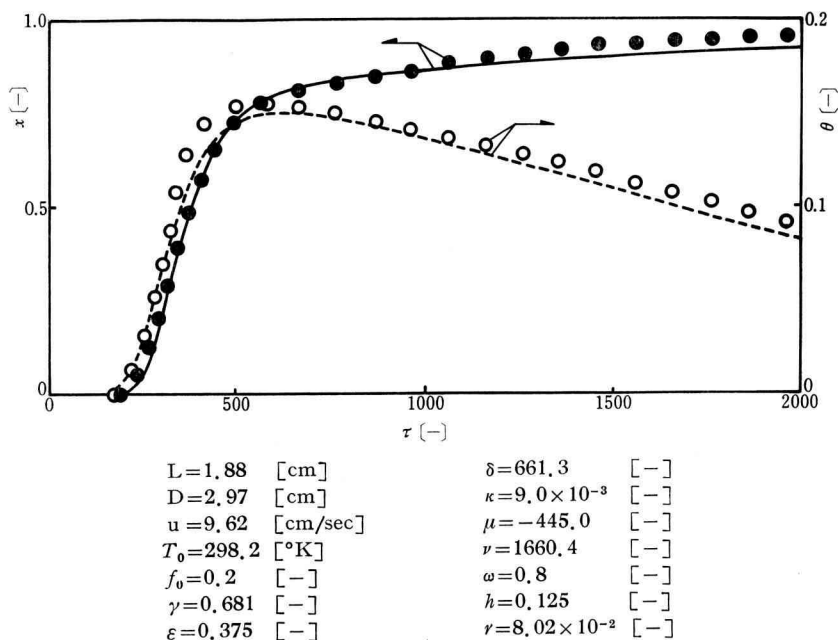


Fig. 8 Comparison of theoretical results with experimental data (Run1)

• } experimental data — } theoretical results
 ○ } - - - }

observation. Values of the experimental heat transfer coefficients and mass transfer coefficients are summarized in **Table 2**.

As temperature or concentration decreases, mass transfer coefficient k_s decreases as well as the value of isothermal case. Furthermore mass transfer coefficient is influenced sensibly by a particle diameter. It is, however, different from isothermal case that as flow rate increases, mass transfer coefficient becomes large. The values of k_s estimated by this model are about 1.3 times as large as that of isothermal case. This is owing to the following reason. Parameters are selected to agree the numerical solutions with the experimental results at the transition region especially, because in the industrial scale, it is necessary to predict a breakthrough time for determination of the cycle time. But there are much temperature rising in that region and mass transfer coefficient is in proportion to the effective diffusivity which increases with the rise of temperature, so the value of k_s becomes fairly large.

As the Reynolds number is large, the value of h_0 becomes large. This tendency is agreed with that of the heat transfer coefficients in the steady state packed bed. The values of h_0 are smaller than those estimated by using Camp-Bells' equation about 10 percents. The values estimated by this model are quite different from those by using Chu-Storrow's equation or Hatta-Maeda's equation, because the conditions of this experimental runs are unsatisfied the assumptions leading the foregoing estimation methods. From another study based on the constant pattern heat transfer zone model,¹⁸⁾ it is noticed that when a

Table 2 Comparison of transfer coefficients estimated by this model with those by the other methods

Run	$k_s a_p \gamma \times 10^2$ [1/sec]		$h_0 \times 10^4$ [cal/cm ² ·sec·deg]			
	Cell-Model	isothermal system	Cell-Model	Hatta-Maeda	Camp-Bell	Chu-Storrow
1	4.61	3.58	3.46	5.94	3.73	18.6
2	5.20	3.56	5.11	6.02	3.83	17.4
3	5.35	3.55	6.14	6.11	3.90	17.7
4	5.13	3.55	6.52	6.49	4.26	21.2
5	5.42	3.58	6.77	6.70	4.44	21.2
6	5.81	4.15	3.56	6.36	3.97	18.9
7	5.83	4.15	4.23	6.66	4.25	22.1
8	9.47	5.15	5.29	6.47	3.91	18.1
9	11.0	5.14	5.86	6.96	4.36	22.8
10	2.18	0.796	3.67	6.66	5.00	8.36
11	2.30	0.798	3.78	6.94	5.23	9.49
12	2.10	0.796	7.10	7.35	5.78	11.8
13	2.37	0.796	5.41	6.88	5.25	17.1
14	2.78	0.796	7.67	7.54	5.99	22.5
15	0.754	0.428	4.01	6.92	4.95	8.87
16	0.832	0.430	4.34	7.32	5.37	11.0

column is long enough, the experimental heat transfer coefficients become close to the values estimated by Chu-Storrow' method.

Conclusions

The cell model approach has been adopted to predict the performance of nonisothermal fixed bed adsorption column and to investigate the effects of several controlling variables. When there is an intensive temperature rising, the spread of breakthrough curve is greater than that would be expected for an isothermal system with the same mass transfer coefficient, and mass transfer coefficients estimated by this nonisothermal model are larger than the value of isothermal model. Thus, when a nonisothermal column is designed on the mass transfer coefficient calculated by correct method but assuming isothermal behaviour, premature breakthrough will occur. Such difficulties may also occur in the scale-up from a small diameter laboratory column to a larger unit. The column diameter is the denominator of the parameter ω , so as diameter is greater, the value of ω becomes smaller and nonisothermal effects will be more pronounced leading to a more diffuse breakthrough curve. So industrial column with large diameter and a large amount of generated heat must be designed not as the isothermal model but as the nonisothermal model, and this cell model seems to be available if the study is developed to the larger column.

Acknowledgment

The author wishes to thank Assistant Professor Kenji Ikeda of Yokohama National

University for suggesting this investigation as well as for constant guidance in the course of the work. Thanks are also due to Professor Terukatsu Miyauchi, University of Tokyo, for his advice and assistance, and also for reading and correcting the manuscript.

Nomenclature

- a : Langmuir equilibrium constant [cm^3/g]
 a_0 : constant in Eq. (5) [cm^3/g]
 a_p : ratio of external area to pellet weight [cm^2/g]
 b : saturated adsorbate concentration in the Langmuir equation [g/g_{ad}]
 b_1 : constant in Eq. (5) [g/g_{ad}]
 b_2 : constant in Eq. (5) [$\text{g}/\text{g}_{ad} \cdot ^\circ\text{K}$]
 B : dimensionless length ($=L/d_p$) [—]
 c : adsorbate concentration in gas phase [g/cm^3]
 c_0 : adsorbate concentration in feed gas [g/cm^3]
 C_{pg} : mean integral heat capacity of the gas mixture [$\text{cal}/\text{g deg}$]
 C_{ps} : heat capacity of the adsorbent [$\text{cal}/\text{g deg}$]
 d_p : diameter of particle [cm]
 D : diameter of bed [cm]
 f : mole fraction of adsorbate in gas phase [—]
 h : dimensionless length of unit cell defined by Eq. (15) ($=L_0/L$ or $1/n$) [—]
 h_0 : overall heat transfer coefficient at column wall [$\text{cal}/\text{cm}^2 \text{ sec deg}$]
 $-\Delta H$: heat of adsorption [cal/mole]
 k_s : solid phase mass transfer coefficient [cm/sec]
 L : length of bed [cm]
 L_0 : length of unit cell [cm]
 n : number of cells [—]
 Pe : Péclet number [—]
 q : adsorbate loading [g/g_{ad}]
 q^* : adsorbate loading in equilibrium with fluid phase concentration c [g/g_{ad}]
 q_0^* : value of q^* at $T=T_0$ and $c=c_0$ [g/g_{ad}]
 r : equilibrium parameter for Langmuir equation defined by Eq. (15)

$$= (1 + a_0 \exp(-\frac{\Delta H}{RT_0}) c_0)^{-1}$$
 [—]
 R : gas constant [$\text{cal}/\text{mole } ^\circ\text{K}$]
 Re_p : Reynolds number [—]
 T : temperature in the bed [$^\circ\text{K}$]
 T_w : temperature of bed wall [$^\circ\text{K}$]
 T_0 : initial temperature [$^\circ\text{K}$]
 t : time [sec]
 u : superficial velocity [cm/sec]
 x : dimensionless gas phase concentration defined by Eq. (14) ($=c/c_0$) [—]
 y : dimensionless solid phase concentration defined by Eq. (14) ($=q/q_0^*$) [—]

Greek Letters

- β : dimensionless parameter defined by Eq. (15) ($=b_2 T_0 / (b_1 - b_2 T_0)$) [—]
 γ : bulk density of the adsorbent [g/cm^3]
 δ : dimensionless parameter defined by Eq. (15) ($=\gamma q_0^* / \epsilon c_0$) [—]
 ϵ : porosity of packed bed [—]
 η : dimensionless equilibrium adsorbate loading defined by Eq. (14) ($=q^*/q_0^*$) [—]
 θ : dimensionless temperature defined by Eq. (14) ($=(T-T_w)/T_w$) [—]
 κ : dimensionless mass transfer coefficient defined by Eq. (15) ($=k_s a_p \gamma L / u$) [—]

- λ : dimensionless parameter defined by Eq. (15) $(= \Delta H / RT_0)$ [—]
 μ : dimensionless parameter defined by Eq. (15) $(= \gamma \Delta H q_0^* / \varepsilon \rho_g C_{pg} T_w)$ [—]
 μ_g : viscosity of fluid [g/cm sec]
 ν : dimensionless parameter defined by Eq. (15) $(= (\varepsilon \rho_g C_{pg} + \gamma C_{ps}) / \varepsilon \rho_g C_{pg})$ [—]
 ρ_g : density of fluid [g/cm³]
 τ : dimensionless time defined by Eq. (14) $(= ut/L)$ [—]
 ω : dimensionless heat loss through the bed wall defined by Eq. (15) $(= 4h_0 L / Du \varepsilon \rho_g C_{pg})$

References

- 1) Meyer, O.W., T.W. Weber, A.I. Ch. E. Journal, **13**, 457 (1967)
- 2) Ruthven, D.M., *Chem. Eng. Sci.*, **30**, 803 (1975)
- 3) Ikeda, K., et al., *Chem. Eng. Sci.*, **28**, 227 (1973)
- 4) Kawazoe, K., et al., *Seisankenkyu*, **21**, 563 (1969)
- 5) Carter, J.W., *Trans. Instn. Chem. Engrs.*, **46**, T222 (1968)
- 6) Leavitt, F.W., T.W. Weber, *A.I. Ch. E. Journal*, **13**, 457 (1967)
- 7) Pan, C.Y., D. Basmadjian, *Chem. Eng. Sci.*, **25**, 1653 (1970)
- 8) Chen, J.W., F.L. Cunningham and J.A. Bulge, *Ind. Eng. Chem. (P.D.D.)*, **11**, 430 (1972)
- 9) Deans, H.A., L. Lapidus, *A.I. Ch. E. Journal*, **6**, 656 (1960)
- 10) Youngok, A., *Iowa State Univ. Ph. D.*, Thesis (1966)
- 11) Kawazoe, K., V.A. Astakhov and T. Kawai, *Seisankenkyu*, **22**, 373 (1970)
- 12) Ikeda, K., et al., *Preprints of the 11th Autumn Meeting of the Soc. of Chem. Engrs., Japan*, **D202** (1977)
- 13) Kawazoe, K., et al., *Kagaku Kogaku*, **30**, 1007 (1966)
- 14) Kawazoe, K., *Kagaku Kogaku*, **31**, 54 (1967)
- 15) Camp-Bell, "Kagaku Kogaku Binran 1st ed." (edited by Soc. of Chem. Engrs., Japan), 174 (1958)
- 16) Chu, Y.C., J.A. Storrow, *Chem. Eng. Sci.*, **1**, 230 (1952)
- 17) Hatta, S., S. Maeda, *Kagaku Kikai*, **12**, 56 (1948)
- 18) Ikeda, K., et al., *Preprints of the 41th Annual Meeting of the Soc. of Chem. Engrs., Japan*, **G306** (1976)